

# Effect of axial temperature gradient on chromatographic efficiency under adiabatic conditions

Krisztián Horváth\*, Szabolcs Horváth, Diána Lukács

*Department of Analytical Chemistry, University of Pannonia, Egyetem utca 10, H-8200 Veszprém, Hungary*

---

## Abstract

The effect of axial temperature gradient on the chromatographic efficiency was studied under adiabatic conditions by a modeling approach. The Equilibrium-Dispersive model of chromatography was used for the calculations. The model was extended by taking into account the axial temperature gradient. The results show that due to the temperature gradient, there are ~~both~~ retention and migration velocity gradients in the column. Since the retention factor,  $k$  is not constant in the column, ~~these~~  $k$  cannot be calculated as the ratio of net retention and hold-up times. As a result of the gradual increase of migration velocity, the retention times of solutes decreases as the slope of temperature gradient increases. In addition, the band in the column have extra broadening due to larger migration velocity of the front of band. The width of bands becomes larger at larger change of temperature. In the same time, however, the release velocity of the compounds from the column is increasing as  $\Delta T$  increases. Accordingly, an apparent peak compression effect makes the peaks thinner. As a result of the two counteracting effects (peak expansion, apparent peak compression) the column efficiency does not change significantly in case of axial temperature gradient under adiabatic conditions. The resolutions, however, decreases slightly due to the decrease of retention times.

*Keywords:* temperature gradient, separation efficiency, adiabatic conditions, Equilibrium-Dispersive model

---

\*Corresponding author, email: [raksi@almos.uni-pannon.hu](mailto:raksi@almos.uni-pannon.hu)

## 8 1. Introduction

9 One of the few possibilities of improving the efficiency of chromatographic separations is  
10 the use of fine particles [1]. By using them, fast mass transfer and high throughputs can be  
11 achieved in analytical laboratories. During the last decades, an active development of packing  
12 materials was undertaken. As a result, the size of a typical particle used in ultra-high perfor-  
13 mance liquid chromatography (UHPLC) decreased from 5.0 to 1.7  $\mu\text{m}$ . Recently [2], a series  
14 of very small core-shell particles (1.0-1.4  $\mu\text{m}$ ) were tested including the smallest commercially  
15 available 1.3  $\mu\text{m}$  core-shell phase[2]. Compared to a 1.7  $\mu\text{m}$  fully porous phase, 20–40% gain  
16 in efficiency were observed by using the 1.3  $\mu\text{m}$  particles. For an UHPLC stationary phase, the  
17 price of the improved separation power is the necessity of high pressure. The viscous friction  
18 of the mobile phase pushed through the chromatographic bed causes enormous resistance to  
19 the flow and requires high inlet pressures [3]. Depending on the length of column, and the  
20 viscosity of mobile phase, operating columns packed with sub-2  $\mu\text{m}$  particles often requires  
21 pressures up to 1000–1200 bar. Due to the law of conservation of energy, the energy applied to  
22 motion finally converts to heat. As a result, both radial and axial temperature gradient form in  
23 the column that affect the overall column performance.

24 In the middle of 70s, Halász et. al studied [4] the limits of high performance liquid chro-  
25 matography. They concluded that temperature gradients existed in axial and radial directions  
26 inside the column due to the frictional heat. As a consequence, they limited the pressure drop,  
27  $\Delta p$ , 500 bar in practical measurements. It was also predicted that the minimum particle size in  
28 HPLC would be between 1 and 3  $\mu\text{m}$ . In the last four decades, several authors studied [5–11]  
29 the formation of axial and radial temperature gradients both experimentally and theoretically.  
30 The main conclusion is that the radial distribution of the temperature causes a radial viscosity  
31 gradient of the mobile phase. The eluent is more viscous in the colder region at the column  
32 wall than in the warmer central region. As a result, the velocity of mobile phase also has a  
33 radial gradient. It flows faster in the central region of the column than close to the colder wall.  
34 Consequently, the shape of bands become parabolic, which decreases of the apparent column  
35 efficiency. Since retention depends on temperature, the radial temperature gradient causes also  
36 a radial distribution of retention factors. The adsorption equilibrium constants decrease with  
37 increasing temperature. Retention of solutes is smaller in the column center than near its wall.  
38 As a result, the migration velocity of solutes relative to the eluent velocity is higher at the col-

39 umn center than at the column wall. This phenomenon further decreases column performance.  
40 Several theoretical approaches were used for simulating the effect of radial temperature gradi-  
41 ent on column efficiency [3, 8, 12–16]. These works confirmed the deteriorating effect of the  
42 radial temperature gradient through both the flow pattern and retention change.

43 A possible solution to overcome the negative effect of radial temperature gradient is the  
44 decrease of efficiency of column thermostat or perfect insulation of the column. It was shown  
45 [17] that the decrease in chromatographic performance is larger in case of water bath than using  
46 a still air heater. The effect of viscous heat generation can be minimized when the temperature  
47 of the column wall is not controlled and the wall remains in contact with still air [18]. The  
48 radial temperature gradient can be diminished or eliminated by insulating the column. Recently,  
49 Gritti et. al [19, 20] developed a cylindrical vacuum chamber in order to isolate thermally the  
50 chromatographic column from the external air environment and to maximize resolution power  
51 in ultra-high performance liquid chromatography. It was shown that less than 1% of the viscous  
52 heat was dissipated to the external air environment. As a result, the amplitude of the radial  
53 temperature gradient is reduced 0.01 K. Improvement in resolution power was observed due to  
54 the uniform distribution of the flow velocity across the column diameter. The eddy dispersion  
55 term in the van Deemter equation was reduced by  $0.8 \pm 0.1$  reduced plate height unit, that is a  
56 significant gain in column performance.

57 For the estimation of separation efficiency of a non-uniform column (varying diameter,  
58 adsorption strength, flow rate, etc.) a general equation was derived by Giddings [21]. It was  
59 shown that the apparent height equivalent to a theoretical plate,  $\bar{H}$ , was affected by both the  
60 variations of the local  $H_s$  and migration velocities. For the calculation of  $\bar{H}$ , a simple equation  
61 was derived. The effect of axial temperature and pressure gradients on column efficiency was  
62 studied by Neue and Kele [22]. The authors analyzed the coefficients of the van Deemter  
63 equation under the idealized condition of complete radial uniformity. It was found that for an  
64 adiabatic column, the overall separation efficiency was not affected significantly up 1000 and  
65 even 2000 bar pressure drops. The authors neglected the effect of retention variation in the  
66 column completely.

67 The aim of this work is the study of effect of axial temperature gradient on the migration  
68 and spreading of solute zones and on the efficiency of chromatographic separations **through**  
69 **axial the change of retention** in adiabatic cases. In this study, theoretical models provide more

70 accurate insight to the chromatographic processes take place in the column than ~~the~~ practical  
71 measurements, since in the latter case other effects can modify the column efficiency as well.  
72 The Equilibrium-Dispersive, ED, model [1] was used for the simulation of chromatographic  
73 runs. The effect of temperature on column efficiency was neglected. By applying the ED  
74 model, efficiencies of separations for different linear temperature gradients are analyzed.

75 **2. Theory**

76 *2.1. Effect of temperature on retention*

77 The dependence of the retention factor,  $k$ , of a compound on the temperature can be de-  
78 scribed by the following equation.

$$k = k_{\infty} \exp\left(-\frac{\Delta H}{R T}\right) \quad (1)$$

79 or in logarithmic form

$$\ln k = -\frac{\Delta H}{R T} + \ln k_{\infty} \quad (2)$$

80 where  $\Delta H$  is the change of molar enthalpy of the system during adsorption,  $R$  the universal  
81 gas constant,  $T$  the absolute temperature, and  $k_{\infty}$  the retention factor of the solute at infinite  
82 temperature.  $k_{\infty}$  is constant and it consists of the change of molar entropy and the phase ratio  
83 of the column. Eq. (2) allows the calculation of the local retention factor in the knowledge of  
84 temperature gradient,  $T(z)$ .

The retention time of the solute can be calculated by the following integral

$$t_R = \int_0^L \frac{u_0}{1 + k(z)} \frac{1 + k(z)}{u_0} dz \quad (3)$$

85 where  $u_0$  is the linear velocity of the eluent, and  $L$  the column length.

86 *2.2. Peak formation*

87 In HPLC, separations take place in space, while the chromatogram is obtained in time  
88 dimension. A chromatographic peak is generated in the following steps:

- 89 1. generation of initial zone,
- 90 2. separation,
- 91 3. generation of chromatogram.

92 The initial solute zone is generated after the injection of a sample plug at the head of chro-  
93 matographic column. The width of the initial solute zone can be calculated as

$$\Delta z = t_{inj} \frac{u_0}{1 + k_{in}} \quad (4)$$

94 where  $\Delta z$  is the width of the zone of solute after injection,  $u_0$  the linear velocity of the eluent,  
 95  $k_{in}$  the retention factor of solute at the column inlet, and  $t_{inj}$  the injection time.

$$t_{inj} = \frac{V_{inj}}{F} \quad (5)$$

96 where  $V_{inj}$  is the injection volume, and  $F$  the flow rate of eluent.

97 In Eq. (4), the conversion factor between time and space is the velocity of the zone. Ac-  
 98 cordingly, the initial width of the zone is smaller if  $k_{in}$  is larger, and vice versa.

99 During the migration through the column, the solute band changes its shape due to mass  
 100 transfer kinetics. If the retention factor of the solute has a gradient in the column, additional  
 101 peak expansion or peak compression can affect the zone width depending on the relative veloc-  
 102 ities of the front and back of the zone.

$$u_{front} = \frac{u_0}{1 + k_{front}} \quad (6)$$

$$u_{back} = \frac{u_0}{1 + k_{back}} \quad (7)$$

103 If  $u_{front} > u_{back}$ , or in other words  $k_{front} < k_{back}$ , extra band broadening takes place in the  
 104 column. The zone widens more than it should be due to the classical band broadening effects.  
 105 When  $k_{front}$  is larger than  $k_{back}$ , however, the zones become thinner due to peak compression.

106 Finally, the zones leaves the column with the release velocity,  $u_{rel}$ , and appears on the  
 107 chromatogram in time scale. The conversion between the space and time dimensions is  $u_{rel}$ .

$$\Delta t_{peak} = \Delta z_{final} \frac{u_0}{1 + k_{rel}} \frac{1 + k_{rel}}{u_0} \quad (8)$$

108 Accordingly, for a given final zone width,  $\Delta z_{final}$ , the peak on a chromatogram is thinner if  
 109 the release velocity is large, and the peak is wider if  $u_{rel}$  is small.

110 Eqs. (4) – (7) suggest that the width of a chromatographic peak is affected significantly  
 111 if there is a gradient of retention factor in the column. The equations, however, did not tell  
 112 anything on the overall column efficiencies.

### 113 2.3. Equilibrium-Dispersive model

114 Under linear conditions, when concentration of analyte injected onto the column is small  
 115 and the rate of adsorption/desorption is infinitely high, the differential mass balance of the

116 solute [1, 21] can be written as:

$$\frac{\partial c(z, t)}{\partial t} + \frac{\partial k(z, t) c(z, t)}{\partial t} = -u_0 \frac{\partial c(z, t)}{\partial z} + D_a \frac{\partial^2 c(z, t)}{\partial z^2} \quad (9)$$

117 where  $c$  is the mobile phase concentration of the compound,  $k$  the retention factor,  $t$  the time,  
118 and  $z$  the distance along the column. Eq. (9) is a local equation, and valid everywhere in the  
119 column.

The apparent dispersion coefficient,  $D_a$ , is given by:

$$D_a = \frac{H u_0}{2} \quad (10)$$

120 where  $H$  is the apparent height equivalent to a theoretical plate (HETP), obtained experimen-  
121 tally. This approximation allows the equilibrium-dispersive model to correctly take into account  
122 the influence of the column efficiency on the profile of elution bands.

123 If the retention factor does not change with time, i.e. the column is under steady-state  
124 condition, Eq. (9) can be rewritten as

$$\frac{\partial c(z, t)}{\partial t} = -u_A \frac{\partial c(z, t)}{\partial z} + \frac{H u_A}{2} \frac{\partial^2 c(z, t)}{\partial z^2} \quad (11)$$

125 where  $u_A$  is the migration velocity of the zone

$$u_A = \frac{u_0}{1 + k(z)} \quad (12)$$

126 By Eq. (11), the effect of temperature gradient on the chromatographic separation can be  
127 simulated and studied rather accurately.

### 128 3. Experimental

129 For the numerical solution of Eq. (11), the Martin-Synge algorithm [23] was used. The  
130 algorithm mimics the Martin-Synge plate model, i.e. a chromatographic system that is discrete  
131 in space and continuous in time. The column is divided for  $N$  number of continuous flow  
132 mixers, where  $N$  is the number of theoretical plates. In each plate, the following ordinary  
133 differential equation was solved with high accuracy.

$$\frac{d c_i[t]}{d t} = -u_A \frac{c_i[t] - c_{i-1}[t]}{\Delta z} \quad (13)$$

134 where  $i$  represents the rank of the plate, ( $0 \leq i \leq N$ ).  $c_0$  and  $c_N$  are the injection and elution  
135 profiles, respectively. The band dispersion is taken into account by the proper choice of  $N$ . The  
136 algorithm can be extended for non-linear conditions, and was used successfully in the solution  
137 of different chromatographic projects [24–27].

138 The calculations were performed using a software written in house in Python program-  
139 ming language (v. 3.5, Anaconda Python Distribution), using the NumPy, SciPy and Numba  
140 packages. The following parameters were set during the calculations:

- 141 • column length,  $L$ , 5 cm,
- 142 • column plate number,  $N$ , 1000,
- 143 • eluent linear velocity,  $u_0$ , 5 cm/min,
- 144 • retention factor at infinite temperature,  $k_\infty$ , 0.165,
- 145 • column head temperature,  $T_{\text{in}}$ , ~~193~~ 293 K,
- 146 • change of molar enthalpy,  $-\Delta H$ , 5000 – 15 000 J/mole (101 levels, stepsize: 100 J/mole),
- 147 • total rise of temperature,  $\Delta T$ , 0 – 50 K (101 levels, stepsize: 0.5 K).

148 It was shown [3] that the axial temperature gradient is close to linear in case of adiabatic  
149 conditions. Accordingly, linear axial temperature gradient was applied during calculations.

$$T(z) = T_{\text{in}} + \Delta T \frac{z}{L} \quad (14)$$



150 Note that 1000 plate numbers was set during the calculations. The dependency of results  
151 on the number of theoretical plates was tested at different  $N$ s up to ~~10000~~.30000. The same  
152 numerical results were observed at each case.

153 50 K increase of temperature can be generated by ~1500 bar pressure drop in case of  
154 methanol, or by ~2500 bar pressure drop in case of water. The latter is far beyond the capacity  
155 of the state of the art UHPLC systems. With certain UHPLC systems, even 1300 bar pressure  
156 can be generated that can heat methanol up by 45 K. Accordingly,  $\Delta T$  was maximized at 50 K.

157 The source code of the Python program can be downloaded from the supplementary mate-  
158 rials.

## 4. Results and discussion

### 4.1. Retention behavior under axial temperature gradient

According to Eq. (2), the retention factor of a solute changes gradually in the column if there is axial temperature gradient. In Fig. 1, the values of retention factor of a solute can be seen at different positions in the column at different temperature gradients. The change of molar enthalpy,  $\Delta H$ , of the compound was set to -10 kJ/mol. It can be seen that the retention factor decreases in the column significantly due to the temperature gradient. At 10°C total temperature rise, the decrease of retention factor is just slightly more than 10%. At 50°C, however, it becomes almost 50%. For a compound with higher or lower  $\Delta H$  the change of retention factor is more or less significant, respectively. An important consequence of this phenomenon is that retention factors of solutes cannot be calculated as the ratio of net retention time and hold-up time when the axial temperature gradient is not negligible. It holds for pressure drops larger than 600 bar typically.

Eq. (12) shows that the local migration velocity depends on the local retention factor. It can be seen in Fig. 2 that the local migration velocities increase gradually in the column in case of an axial temperature gradient. The level of increase depends on the total axial change of temperature. The relative migration velocity increases by 10–70% as  $\Delta T$  increases by 10–50°C, respectively. It is important to note that the release velocity is always higher than the initial velocity in case of a positive axial temperature gradient. The migration of compounds shows acceleration during analysis.

As ~~a result of the migration velocity gradient~~ Eq. (3) suggests, the retention times of solutes affected by the axial temperature gradient ~~as well as Eq. (3) suggests~~ due to the gradually varying migration velocities. In Fig. 3, the retention times can be seen as a function of  $\Delta H$  and  $\Delta T$ . The figure highlights that the relative decrease of retention times are higher at larger  $\Delta T$  values. The increasing  $\Delta H$  makes the compound more sensitive toward the axial temperature gradient.

### 4.2. Peak formation under axial temperature gradient

As it was shown in the Theory section, peak formation is affected not just by the mass transfer kinetics but the gradient of migration velocity as well. First, depending on the sign of the derivative of velocity gradient, zone compression or zone expansion can occur in the column

189 during migration. In case of a rising axial temperature, the slope of the velocity gradient is pos-  
190 itive. As a result, the fronts of the peaks always move faster than the back parts. Accordingly,  
191 the zones at the end of the column become wider than they would normally be due to the mass  
192 transfer kinetics. In Fig. 4, the physical width of solute zones at the end of the column can be  
193 seen. Fig. 4 concludes the previous reasoning. The zones become wider if  $\Delta T$  is larger. This  
194 effect is more significant at larger  $\Delta H$  values than at smaller ones.

195 The zone expansion in the column does not necessarily results in wider chromatographic  
196 peaks. As it was shown by Eq. (8), peak widths affected also by the release velocity,  $u_{rel}$ .  
197 In case of a positive temperature gradient, the release velocities are always larger than any  
198 migration velocity in the column. Fig. 5 shows the release velocities of solutes from the column  
199 at different  $\Delta T$  and  $\Delta H$  values. Significant increase in  $u_{rel}$  can be observed at larger temperature  
200 changes than at smaller ones. As in the case of zone widths, the change in release velocity  
201 increases as  $\Delta H$  increases (becomes more negative).

202 It is important to note, that the release velocities are affected more significantly than the  
203 zone widths, suggesting that the chromatographic peaks become thinner due to the positive  
204 axial temperature gradient. Fig. 6 confirms this phenomenon. It can be seen that the chromato-  
205 graphic peaks can be thinner as the axial temperature change increases. This effect is more  
206 significant at larger (more negative)  $\Delta H$  values.

#### 207 4.3. *Effect of axial temperature gradient on chromatographic efficiency*

208 In the previous section it was shown that the chromatographic peak widths decreases due  
209 to the axial temperature gradient in the column (see Fig. 6). Fig. 3, however, showed that the  
210 retention times decreases similarly to the peak widths. Since the number of theoretical plates  
211 depends on the ratio of these two measures, it can be predicted that the apparent number of  
212 theoretical plates are not affected by the axial temperature gradient. Fig. 7 confirms this pre-  
213 diction. It can be seen that the number of theoretical plates do not change significantly due to  
214 the axial temperature gradient. Even at the most extreme case ( $\Delta H = -15$  kJ/mol,  $\Delta T = 50$  K),  
215 the loss of apparent efficiency is less than 6%. Accordingly, by insulating a chromatographic  
216 column, one can keep its efficiency.

217 Giddings [21] derived a simplified equation for the calculation of apparent efficiencies in  
218 case of non-uniform column. When the efficiency is constant throughout the column, the  
219 relative efficiency can be calculated as:

$$\frac{N_{\text{app}}}{N} = \frac{\left( \frac{1}{L} \int_0^L \frac{1+k}{u_0} dz \right)^2}{\frac{1}{L} \int_0^L \left( \frac{1+k}{u_0} \right)^2 dz} \quad (15)$$

220 where  $N_{\text{app}}$  is the apparent number of theoretical plates. In Eq. (15),  $k$  can be calculated by  
 221 Eq. (1).

222 The differences between the results presented in Fig. 7 and calculated by Eq. (15) were  
 223 less than 0.2% in each case (less than 0.049% in average). It confirms the validity of results  
 224 presented in Figs. 1–7 and the proper choice of calculation parameters.

225 In chromatography, analyst need resolution not plate number. It is well known that the  
 226 chromatographic resolution,  $R_s$ , depends on the number of theoretical plates,  $N$ , the difference  
 227 and the sum of retention times.

$$R_s = \frac{\sqrt{N}}{2} \frac{\Delta t_R}{t_{R,1} + t_{R,2}} = \frac{\sqrt{N}}{2} \frac{\alpha - 1}{\alpha + 1 + \frac{2}{k_1}} \quad (16)$$

228 where  $k_1$  is the apparent retention factor, and it is defined as  $\frac{t_{R,1}-t_0}{t_0}$ , and  $\alpha$  is the apparent selec-  
 229 tivity, that is the ratio of the apparent retention factors.

230 Close examination of Eq. (16) and Fig. 7 highlights that the resolutions in case of axial tem-  
 231 perature gradients are not affected through the change of number of theoretical plates.  $R_s$ , how-  
 232 ever, can be affected through selectivity,  $\alpha$ , and retention,  $k_1$ . Depending on the difference of  
 233 molar changes of enthalpy,  $\Delta H$ s, of the two compounds, the selectivities can also be improved  
 234 and deteriorated. If  $\Delta H$  of the first eluting compound is larger than that of the second one, its  
 235 retention time decreases more than that of the first one (see Fig. 3). As a result,  $\alpha$  increases  
 236 due to the axial temperature gradient. If  $\Delta H$  of the second compound is larger,  $\alpha$  decreases.  
 237 Accordingly, a general rule cannot be stated for how selectivities change due to the axial tem-  
 238 perature gradient. Fig. 3, however, showed that retention times can change significantly due to  
 239 the axial temperature gradient. Therefore, resolutions can be decreased through the retention.  
 240 It is important to note however, that the decrease of  $R_s$  depends on the absolute value of  $k_1$  not  
 241 its relative decrease. Eq. (16) is a concave saturation function (just like Langmuir isotherm).  
 242 Its derivative is

$$\frac{dR_s}{dk_1} = \frac{\sqrt{N}(\alpha - 1)}{[2 + k_1(\alpha + 1)]^2} \quad (17)$$

243 that is always positive and continuously decreasing. As a consequence, the decrease of retention  
244 has more significant effect if  $k$  is small. This phenomenon can be seen in Fig. 8. The figure  
245 shows clearly that a modest decrease in resolution can be observed due to the axial temperature  
246 gradient. The degree of resolution loss is negligible. Even in the most extreme case it is less  
247 than 10%, that is less than the accuracy of determination of  $R_s$  according to our experience.

## 248 5. Conclusions

249 The formation of a chromatographic peak, including its final position and shape, is affected  
250 by the retention of the solute significantly. In case of a linear axial temperature gradient, the  
251 front of the solute zones migrate faster than their rear part. As a result, extra peak broadening  
252 takes place in the column. In the same time, however, the high release velocities compensates  
253 this broadening practically. Neither the number of theoretical plates nor the resolutions are af-  
254 fected significantly by the axial temperature gradient. It means, that by insulating a chromato-  
255 graphic column, one can keep its separation power. Because of the gradual change of retention  
256 factors, the measure ~~calectulates~~ calculated as the ratio of net retention  $(t_R - t_0)$  and hold-up times  
257  $(t_0)$  is not the retention factor and does not have any significant physical meaning.

## 258 Acknowledgment

259 This work was supported by the Hungarian Scientific Research Fund (OTKA PD 104819).  
260 Krisztián Horváth acknowledges the financial support of the János Bolyai Research Scholarship  
261 of the Hungarian Academy of Sciences.

262 **References**

- 263 [1] G. Guiochon, A. Felinger, D. G. Shirazi, A. M. Katti, *Fundamentals of Preparative and*  
264 *Nonlinear Chromatography*, Academic Press, Amsterdam, 2006.
- 265 [2] A. Sanchez, G. Friedlander, S. Fekete, J. Anspach, D. Guillarme, M. Chitty, T. Farkas,  
266 *Pushing the performance limits of reversed-phase ultra high performance liquid chro-*  
267 *matography with 1.3  $\mu\text{m}$  core-shell particles*, *J. Chromatogr. A* 1311 (2013) 90–97.
- 268 [3] K. Kaczmarek, F. Gritti, G. Guiochon, *Prediction of the influence of the heat generated*  
269 *by viscous friction on the efficiency of chromatography columns*, *J. Chromatogr. A* 1177  
270 (2008) 92–104.
- 271 [4] I. Halász, R. Endeke, J. Asshauer, *Ultimate limits in high-pressure liquid chromatography*,  
272 *J. Chromatogr. A* 112 (1975) 37–60.
- 273 [5] H. Poppe, J. Kraak, J. Huber, J. van den Berg, *Temperature gradients in HPLC columns*  
274 *due to viscous heat dissipation*, *Chromatographia* 14 (1982) 515–523.
- 275 [6] T. Welsch, M. Schmid, J. Kutter, A. Kálmán, *Temperature of the eluent: A neglected tool*  
276 *in high-performance liquid chromatography?*, *J. Chromatogr. A* 728 (1996) 299–306.
- 277 [7] A. Brandt, G. Mann, W. Arlt, *Temperature gradients in preparative high-performance*  
278 *liquid chromatography columns*, *J. Chromatogr. A* 769 (1997) 109–117.
- 279 [8] A. de Villiers, H. Lauer, R. Szucs, S. Goodall, P. Sandra, *Influence of frictional heating*  
280 *on temperature gradients in ultra-high-pressure liquid chromatography on 2.1 mm i.d.*  
281 *columns*, *J. Chromatogr. A* 1113 (2006) 84–91.
- 282 [9] F. Gritti, G. Guiochon, *Complete temperature profiles in ultra-high-pressure liquid chro-*  
283 *matography columns*, *Anal. Chem.* 80 (2008) 5009–5020.
- 284 [10] K. Kaczmarek, J. Kostka, W. Zapała, G. Guiochon, *Modeling of thermal processes in*  
285 *high pressure liquid chromatography. I. Low pressure onset of thermal heterogeneity*, *J.*  
286 *Chromatogr. A* 1216 (2009) 6560–6574.

- 287 [11] K. Kaczmarski, F. Gritti, J. Kostka, G. Guiochon, Modeling of thermal processes in high  
288 pressure liquid chromatography. II. Thermal heterogeneity at very high pressures, *J. Chromatogr. A* 1216 (2009) 6575–6586.  
289
- 290 [12] H. Poppe, J. Kraak, Influence of thermal conditions on the efficiency of high-performance  
291 liquid chromatographic columns, *J. Chromatogr. A* 282 (1983) 399–412.
- 292 [13] O. Dapremont, G. Cox, M. Martin, P. Hilaireau, H. Colin, Effect of radial gradient of tem-  
293 perature on the performance of large-diameter high-performance liquid chromatography  
294 columns. I. Analytical conditions, *J. Chromatogr. A* 796 (1998) 81–99.
- 295 [14] F. Gritti, G. Guiochon, Effects of the thermal heterogeneity of the column on chromato-  
296 graphic results, *J. Chromatogr. A* 1131 (2006) 151–165.
- 297 [15] G. Desmet, Theoretical calculation of the retention enthalpy effect on the viscous heat  
298 dissipation band broadening in high performance liquid chromatography columns with a  
299 fixed wall temperature, *J. Chromatogr. A* 1116 (2006) 89–96.
- 300 [16] F. Gritti, M. Martin, G. Guiochon, Influence of viscous friction heating on the efficiency  
301 of columns operated under very high pressures, *Anal. Chem.* 81 (2009) 3365–3384.
- 302 [17] M. Fallas, M. Hadley, D. McCalley, Practical assessment of frictional heating effects  
303 and thermostat design on the performance of conventional ( $3\ \mu\text{m}$  and  $5\ \mu\text{m}$ ) columns in  
304 reversed-phase high-performance liquid chromatography, *J. Chromatogr. A* 1216 (2009)  
305 3961–3969.
- 306 [18] F. Gritti, G. Guiochon, Optimization of the thermal environment of columns packed with  
307 very fine particles, *J. Chromatogr. A* 1216 (2009) 1353–1362.
- 308 [19] F. Gritti, M. Gilar, J. Jarrell, Quasi-adiabatic vacuum-based column housing for very high-  
309 pressure liquid chromatography, *J. Chromatogr. A* 1456 (2016) 226–234.
- 310 [20] F. Gritti, M. Gilar, J. Jarrell, Achieving quasi-adiabatic thermal environment to maximize  
311 resolution power in very high-pressure liquid chromatography: Theory, models, and ex-  
312 periments, *J. Chromatogr. A* 1444 (2016) 86–98.
- 313 [21] J. C. Giddings, *Dynamics of Chromatography*, M. Dekker, New York, 1965.



- 314 [22] U. Neue, M. Kele, Performance of idealized column structures under high pressure, J.  
315 Chromatogr. A 1149 (2007) 236–244.
- 316 [23] K. Horváth, J. Fairchild, K. Kaczmarski, G. Guiochon, Martin-synge algorithm for the so-  
317 lution of equilibrium-dispersive model of liquid chromatography, J. Chromatogr. A 1217  
318 (2010) 8127–8135.
- 319 [24] P. Vajda, A. Felinger, Multilayer adsorption on fractal surfaces, J. Chromatogr. A 1324  
320 (2014) 121–127.
- 321 [25] J. Xu, X. Jiang, J. Guo, Y. Chen, W. Yu, Competitive adsorption equilibrium model with  
322 continuous temperature dependent parameters for naringenin enantiomers on chirapak ad  
323 column, J. Chromatogr. A 1422 (2015) 163–169.
- 324 [26] K. Horváth, A. Felinger, Influence of particle size and shell thickness of core-shell pack-  
325 ing materials on optimum experimental conditions in preparative chromatography, J.  
326 Chromatogr. A 1407 (2015) 100–105.
- 327 [27] L. Jeong, R. Sajulga, S. Forte, D. Stoll, S. Rutan, Simulation of elution profiles in liquid  
328 chromatography i: Gradient elution conditions, and with mismatched injection and mobile  
329 phase solvents, J. Chromatogr. A 1457 (2016) 41–49.

330 **Figure captions**

Figure 1: Retention factor of a solute at different positions in the column in case of  $\Delta H = -10$  kJ/mol at different temperature gradients,  $\Delta T$ s: blue - 10K, green - 20K, red - 30K, light blue - 40K, purple - 50K.

Figure 2: Relative migration velocity of a solute at different positions in the column in case of  $\Delta H = -10$  kJ/mol at different temperature gradients,  $\Delta T$ s: blue - 10K, green - 20K, red - 30K, light blue - 40K, purple - 50K.

Figure 3: Retention times as a function of change of molar enthalpy,  $\Delta H$ , and axial temperature.

Figure 4: Physical width of zones at the end of the column at different temperature and enthalpy changes.

Figure 5: Release velocities of solutes from the column at different temperature and molar enthalpy changes.

Figure 6: Chromatographic peak widths at different temperature and enthalpy changes.

Figure 7: Change of chromatographic efficiencies due to axial temperature gradient as a function of changes of molar enthalpy and total temperature in the column.

Figure 8: Change of resolution in effect of axial temperature gradient.

Figure 1

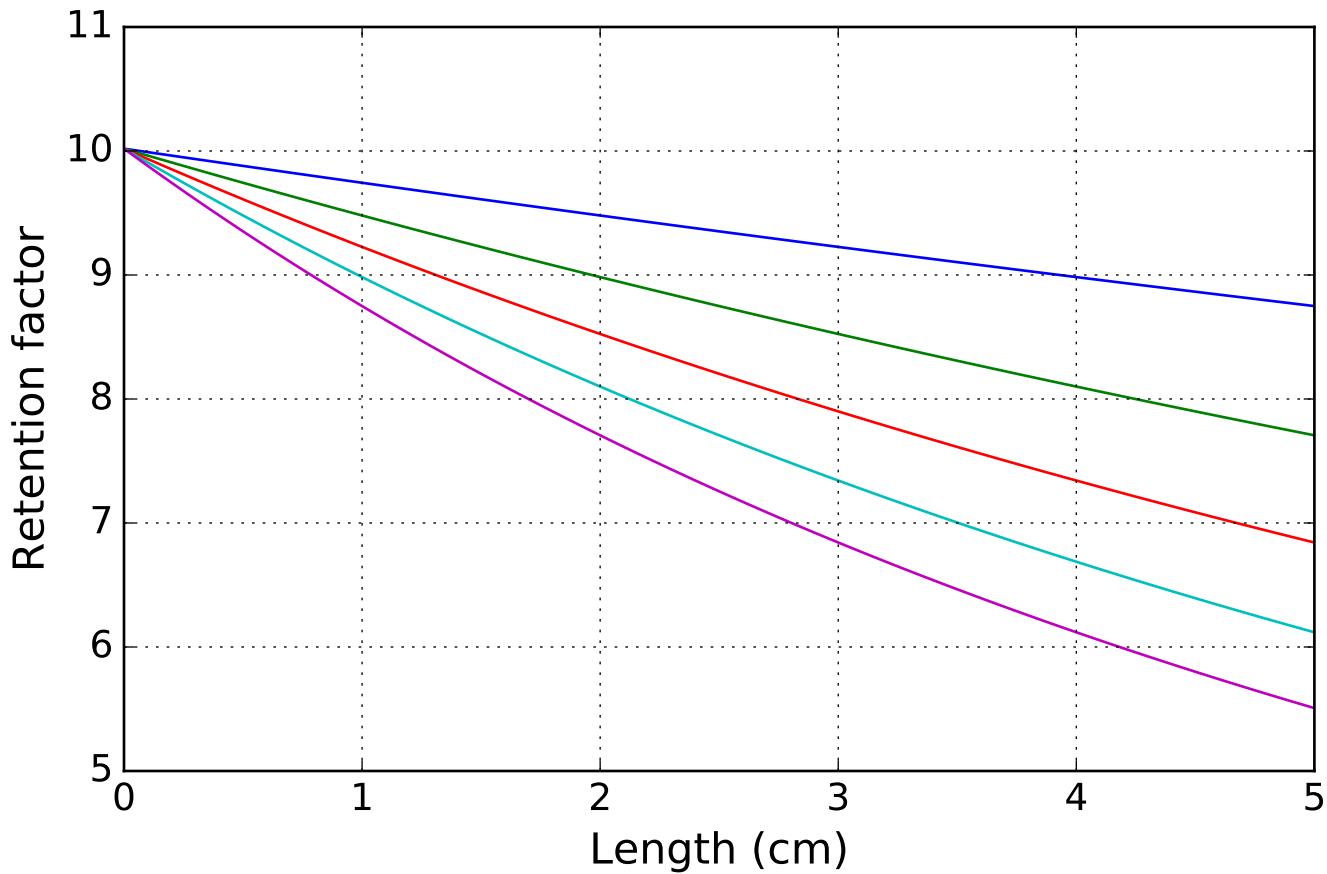


Figure 2

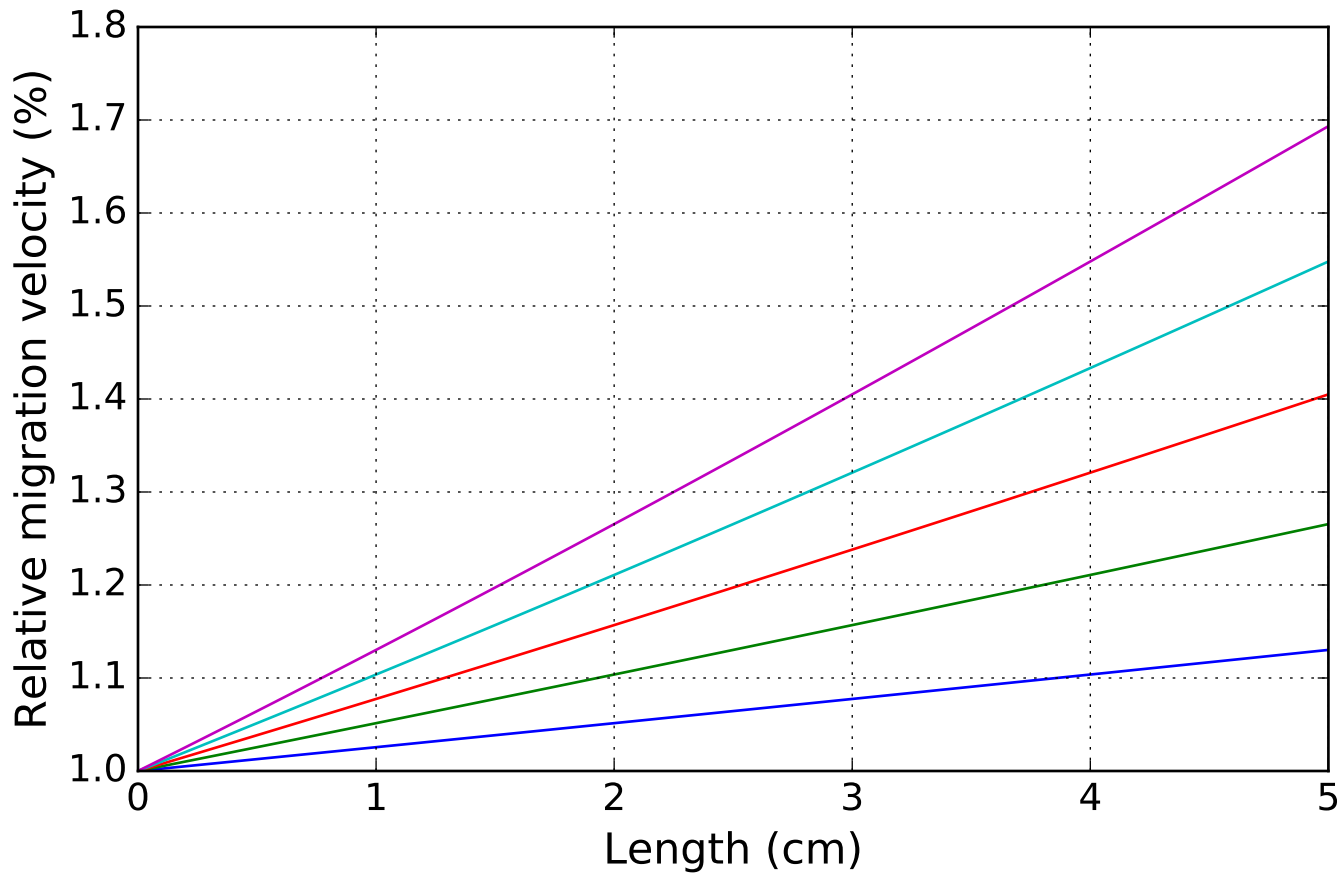


Figure 3

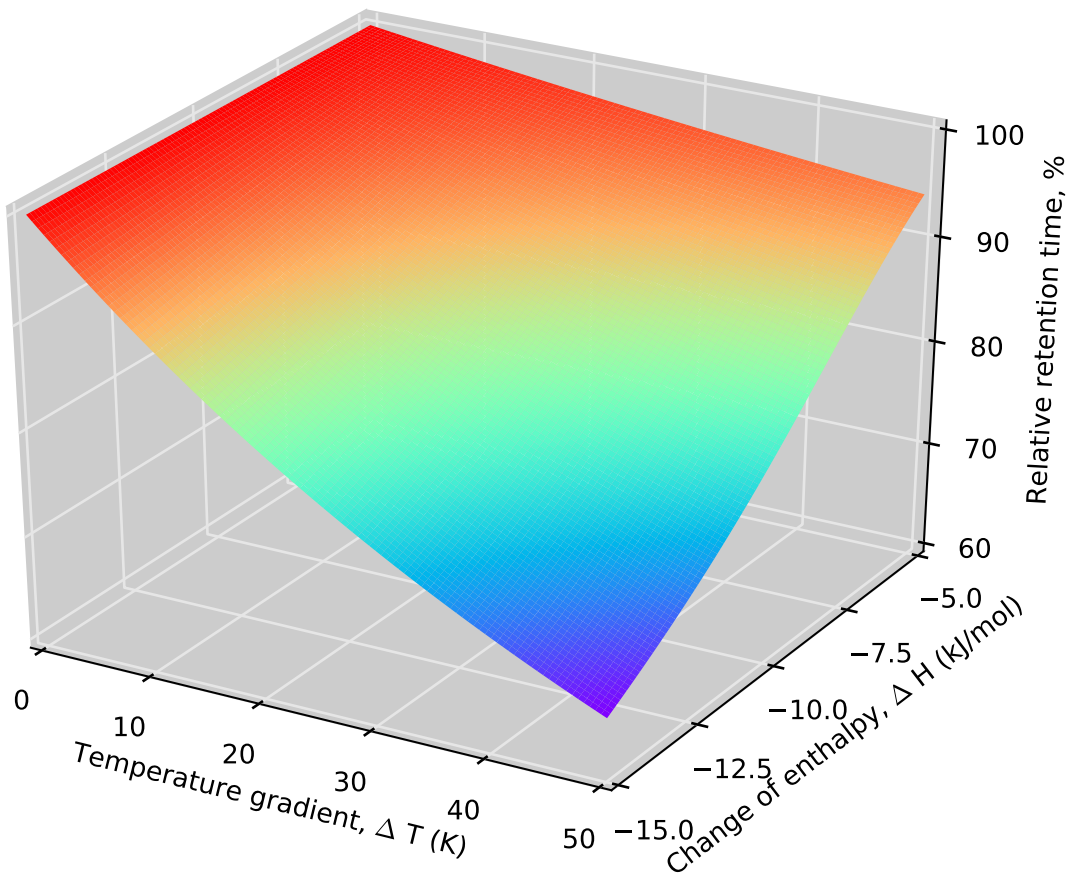


Figure 4

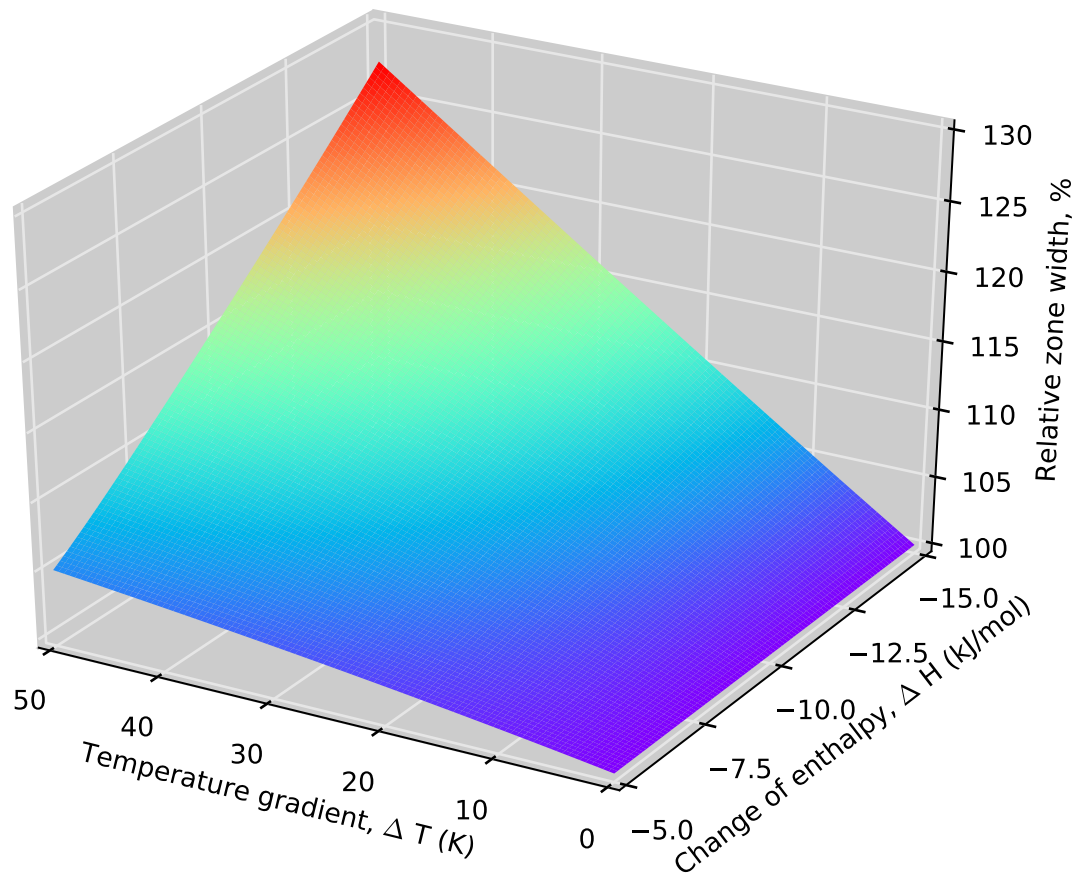


Figure 5

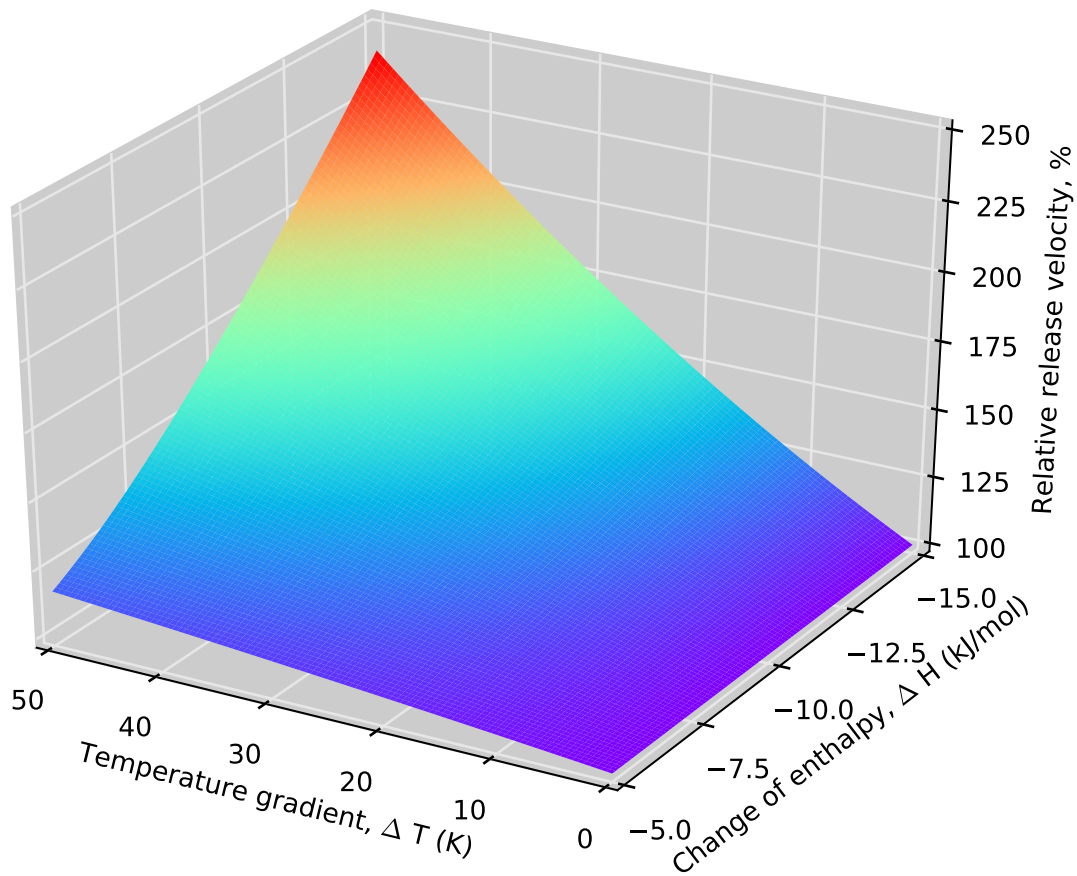


Figure 6

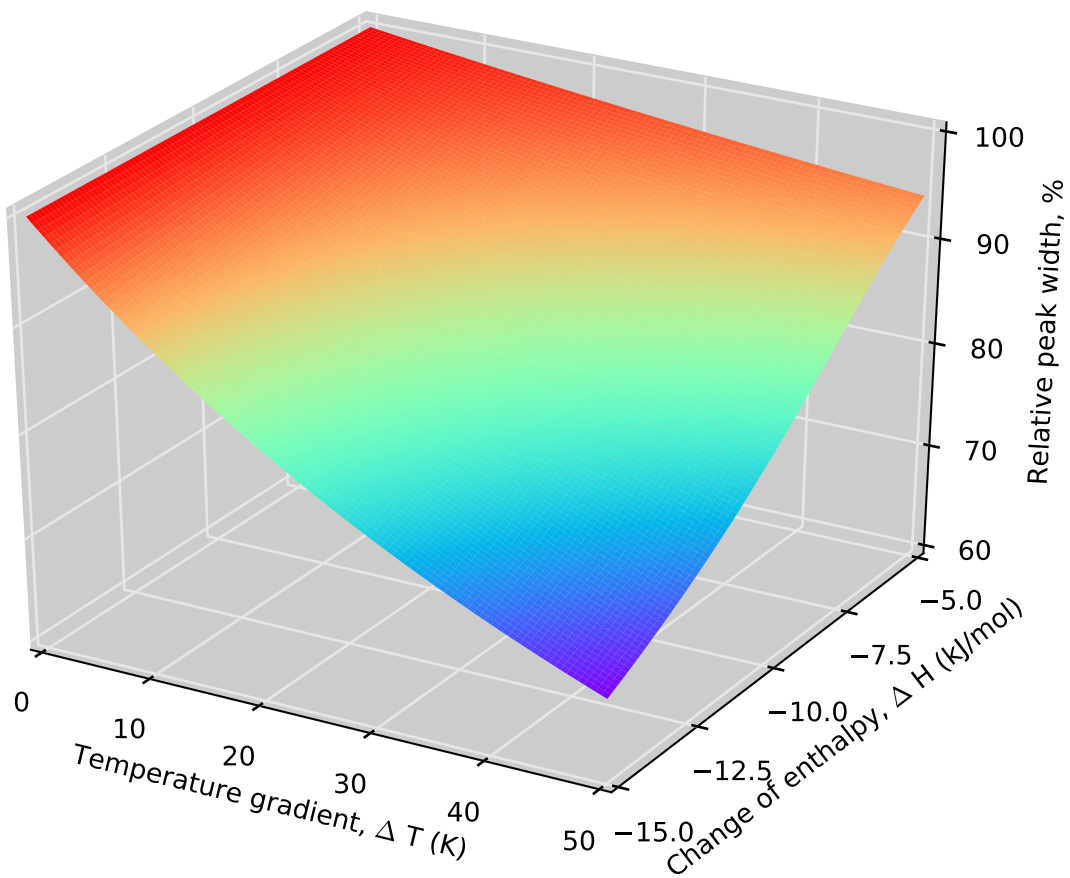




Figure 7

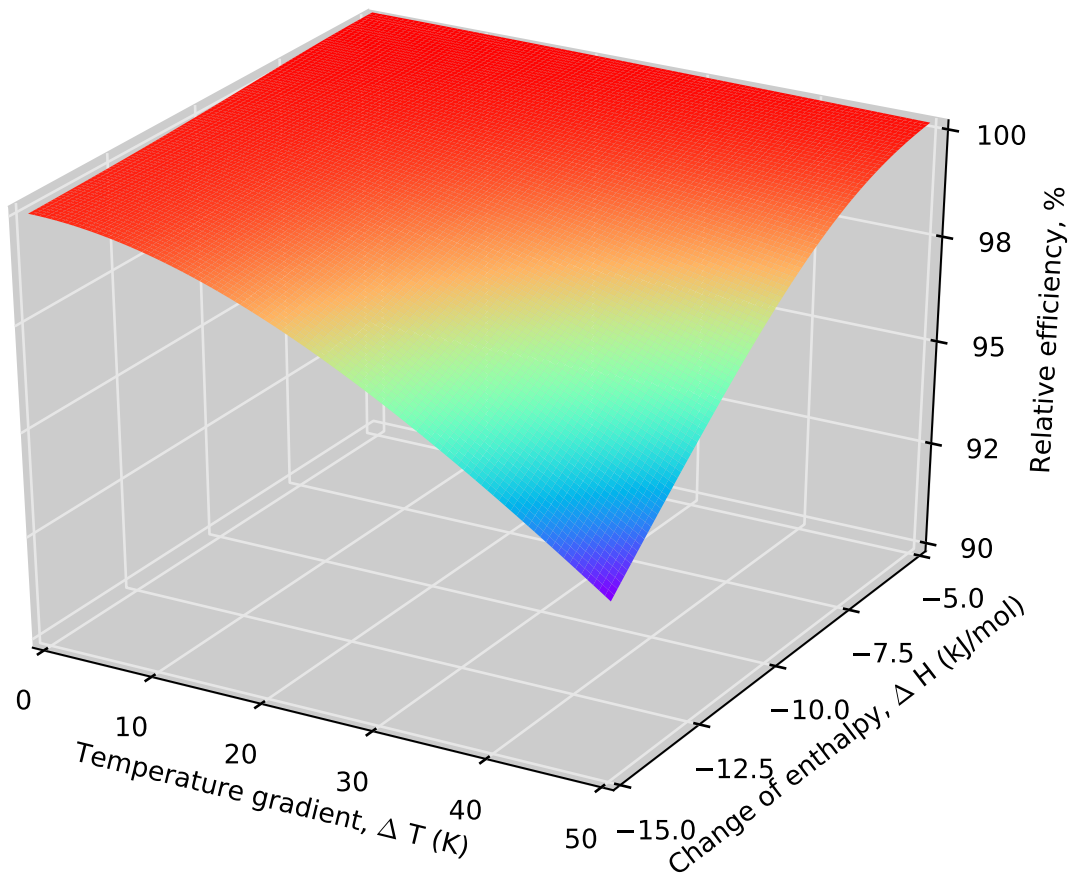


Figure 8

